Induced freezing and re-entrant melting in the hard-disc fluid; applications of the fundamental measure functional

2002 J. Phys.: Condens. Matter 14 12021

(http://iopscience.iop.org/0953-8984/14/46/310)

INSTITUTE OF PHYSICS PUBLISHING JOURNAL OF PHYSICS: CONDENSED MATTER

J. Phys.: Condens. Matter **14** (2002) 12021–12030 PII: S0953-8984(02)37897-4

Induced freezing and re-entrant melting in the hard-disc fluid; applications of the fundamental measure functional

Lasse L Rasmussen and David W Oxtoby

The James Franck Institute, The University of Chicago, 5640 S. Ellis Ave., Chicago, IL 60637, USA

Received 10 June 2002, in final form 8 July 2002
Published 8 November 2002
Online at stacks.iop.org/JPhysCM/14/12021

Abstract

A fundamental measure functional is used to study the induced freezing and re-entrant melting for the hard-disc fluid in an external periodic potential. The phase diagram obtained shows good agreement with recent experimental studies. We also use the functional to describe the hard-disc fluid density near a hard wall and investigate whether this 2D functional can correctly describe the 0D limit.

1. Introduction

It has been known for some years now that colloidal particles in two dimensions can undergo freezing and re-entrant melting when exposed to a one-dimensional periodic potential. As these phenomena were first explored using lasers, they have been named laser-induced freezing (LIF) and laser-induced melting (LIM). Within the last decade several studies have been undertaken using experiments [1–5], simulations [6–9] and theory [10–12] to explore the nature of these phase transitions. The existence of a critical point in the phase diagram, the density ranges in which LIF and LIM occur and how strong an external potential is needed to obtain these phenomena are all subjects still under investigation.

Our understanding of LIF and LIM at the microscopic level is still limited. The prevailing explanation argues that particle fluctuations play an important role in the phase transition as the re-entrant liquid phase can be seen as stripes of particles confined by the external potential where the correlations between stripes are lost.

Almost simultaneously with these discoveries, Rosenfeld [13] constructed a density functional theory to describe hard-particle fluids employing an entirely new type of functional called the fundamental measure functional. This functional has yielded very accurate results for a range of liquid properties, including phenomena only observed in inhomogeneous and confined systems [14–18]. Within the last few years the fundamental measure functional has been successfully applied to more complicated systems such as liquid mixtures [15, 19–21] and particles with anisotropic shapes [22, 23]. Perhaps the most intriguing aspect of Rosenfeld's

theory is that the only input to the functional is the geometric measures or shapes of the particles. Most other types of functional rely on knowledge of particle correlation functions; by contrast to these functionals, the correlation functions fall out naturally from the Rosenfeld functional. This is particularly useful when investigating inhomogeneous systems, where particle correlation functions are generally unknown.

Despite these successful applications of the theory, the functional was initially unable to reproduce the well-known freezing of hard spheres [16, 17, 24]. This led to the development of several extensions to the theory focusing on describing the properties of dimensional crossover correctly [24–27]. But to our knowledge, the original functional has not yet been applied to freezing in 2D.

In this paper we investigate the hard-disc system under the influence of a periodic external potential using Rosenfeld's functional. We are able to confirm several observations seen in recent experiments performed by Bechinger *et al* [5] and provide some support for the proposed explanation behind LIM. Previous theoretical and simulation studies have not produced the phase diagram observed in [5]. We also apply the functional to the case of adsorption at a hard wall, which serves as an excellent test for any theory describing simple liquids.

The phase behaviour of the true 2D hard-disc system is not as well understood as the corresponding 3D system. Size effects play a much larger role in 2D, so recent simulation studies have used larger numbers of particles even than experiment [28], but still have not been able to distinguish definitely between a first-order and a second-order (hexatic) transition. Our density functional approach, being mean field in character, is unable to resolve this issue, but in the presence of an external field it appears to give useful results.

The outline of this paper is as follows. In section 2 we briefly describe the density functional theory used. In section 3, this theory is applied to a hard-disc fluid in different inhomogeneous situations; near a hard wall, in the 0D limit and in a periodic external potential. In section 4, we summarize and comment on the results.

2. Theory

Within density functional theory we calculate the grand-canonical potential Ω as a functional of the one-particle density $\rho(\boldsymbol{r})$. It is related to the Helmholtz free energy F through a Legendre transformation. Since the ideal contribution to F is known exactly, we can write

$$\Omega[\rho(\boldsymbol{r})] = F[\rho(\boldsymbol{r})] + \int \mathrm{d}\boldsymbol{r}\, \rho(\boldsymbol{r}) V_{\mathrm{ext}}(\boldsymbol{r}) - \int \mathrm{d}\boldsymbol{r}\, \rho(\boldsymbol{r})\mu \tag{1}$$

$$F[\rho(\boldsymbol{r})] = \beta^{-1} \int \mathrm{d}\boldsymbol{r}\, \rho(\boldsymbol{r})\{\ln(\Lambda^2 \rho(\boldsymbol{r})) - 1\} + F_{\mathrm{ex}}[\rho(\boldsymbol{r})] \tag{2}$$

where F_{ex} is the non-ideal or excess contribution to F, $V_{\mathrm{ext}}(\boldsymbol{r})$ is an external potential and μ is the chemical potential. β is $1/k_{\mathrm{B}}T$ and Λ is the thermal de Broglie wavelength.

To obtain a proper description of the liquid and solid states, we use the Rosenfeld or fundamental measure theory functional [13]. In particular, we employ the Kierlik–Rosinberg (KR) version [16, 17], which has been shown to be identical to the original Rosenfeld functional [29, 30], but has for our particular purpose a simpler mathematical structure. This functional rests on the assumption that F_{ex} can be described as a functional of a set of weighted densities obtained by averaging the particle density with geometric measures of the particles. This assumption is based on the knowledge of the exact functional, whose behaviour is known in the low- and high-density limits. The excess free energy takes the following form:

$$\beta F_{\mathrm{ex}}[\rho(\boldsymbol{r})] = \int \mathrm{d}\boldsymbol{r}\, \Phi\{n_\gamma(\boldsymbol{r})\} \tag{3}$$

where Φ in any dimension D is given as a function of a set of $D+1$ weighted densities $\{n_\gamma(\boldsymbol{r})\}$. There are several ways to define Φ and the weighted densities, but in 2D the KR version has the following structure:

$$\Phi = -n_0 \ln(1-n_2) + \frac{n_1^2}{4\pi(1-n_2)} \tag{4}$$

and the weighted densities are determined by averages or convolutions of the particle density:

$$n_\gamma(\boldsymbol{r}) = \int \mathrm{d}\boldsymbol{r}'\, \rho(\boldsymbol{r}')\omega^{(\gamma)}(\boldsymbol{r}-\boldsymbol{r}'). \tag{5}$$

The weight functions $\omega^{(\gamma)}(\boldsymbol{r})$ are found by decomposing the Mayer function in pairwise products of functions characteristic of the particles. This decomposition is exact for hard spheres (3D) and hard rods (1D), but represents an approximation for hard discs as discussed in [15]. This yields the following weight functions:

$$\begin{aligned} \omega^{(2)}(r) &= \Theta(R-r) \\ \omega^{(1)}(r) &= \delta(R-r) \\ \omega^{(0)}(r) &= \frac{1}{4\pi}\left(\frac{1}{R}\delta(R-r) + \delta'(R-r)\right). \end{aligned} \tag{6}$$

In Fourier space,

$$\begin{aligned} \omega^{(2)}(k) &= RJ_1(kR)/k \\ \omega^{(1)}(k) &= RJ_0(kR) \\ \omega^{(0)}(k) &= \frac{1}{4\pi}(2J_0(kR) - kRJ_1(kR)). \end{aligned} \tag{7}$$

Given a free energy functional, the standard procedure for solving for the equilibrium density distribution is to minimize the grand-canonical potential at constant pressure and temperature. Setting $\frac{\delta\Omega[\rho(\boldsymbol{r})]}{\delta\rho(\boldsymbol{r})} = 0$ the following equation is obtained:

$$\rho(\boldsymbol{r}) = \rho_0 \exp(-\beta V_{\mathrm{ext}}(\boldsymbol{r}) + c_1(\rho:\boldsymbol{r}) - c_1(\rho_0:\boldsymbol{r})) \tag{8}$$

where $c_1(\rho:\boldsymbol{r}) = -\frac{\delta\beta F_{\mathrm{ex}}[\rho(\boldsymbol{r})]}{\delta\rho(\boldsymbol{r})}$ is the one-particle direct correlation function. $c_1(\rho_0:\boldsymbol{r})$ is the corresponding function for the bulk fluid. To ensure that equation (8) remains normalized, it is divided by $\int \mathrm{d}\boldsymbol{r}\,\rho(\boldsymbol{r})$. Taking this together with equations (3) and (5), we obtain

$$c_1(\rho:\boldsymbol{r}) = -\int \mathrm{d}\boldsymbol{r}' \sum_\gamma \frac{\delta\Phi}{\delta n_\gamma(\boldsymbol{r}')}\omega^{(\gamma)}(\boldsymbol{r}-\boldsymbol{r}') \tag{9}$$

which can be calculated numerically using FFT. Equations (8) and (9) can be solved self-consistently for the equilibrium density $\rho(\boldsymbol{r})$.

This recipe is in principle sufficient for calculating the equilibrium density distribution and the associated free energy, given the form of $V_{\mathrm{ext}}(\boldsymbol{r})$. However, in the case of a solid, the density distribution is usually highly peaked around the lattice sites, and solving for it self-consistently is a daunting numerical task. Instead, we use the well-known method of approximating the solid density as a sum of Gaussian distributions over the lattice sites:

$$\rho(\boldsymbol{r}) = \rho_0 \sum_i \frac{\alpha}{\pi}\exp(-\alpha(\boldsymbol{r}-\boldsymbol{r}_i)^2) \tag{10}$$

where ρ_0 is the average density and $\boldsymbol{r}_i$ denotes the position of the lattice sites. α determines the width of the distribution and is used as a variational parameter when minimizing the free energy. We use a triangular lattice to model the solid.

The equilibrium density distribution is ultimately determined by the external potential. Much of the interest in the field is focused on a periodic 1D potential, since this has been shown

experimentally to induce freezing. Furthermore, recent studies [3–5, 7, 9] have indicated a re-entrant perturbed liquid phase when the 1D potential becomes sufficiently strong. In order for the 1D potential to be commensurate with the triangular lattice it must possess a certain periodicity and is modelled using the following form:

$$V_{\text{ext}}(x) = V_0 \cos(2\pi x/L) \tag{11}$$

where the period L is given by $L = a\sqrt{3}/2$ with a the lattice constant. The cosine is an excellent fit to the external potential created in experiments.

3. Results

The main purpose of this paper is to investigate the phenomena of induced freezing and melting in simple liquids, but we first present two important test cases for the functional in order to justify using it in 2D. Both cases have been studied in 3D using the Rosenfeld and other functionals, but studies have to our knowledge not been carried out for the hard-disc fluid so far within in the framework of DFT.

3.1. Adsorption at a hard wall

Solving for the density profile of a bulk liquid in the presence of a hard wall constitutes an excellent test for a functional used to model an inhomogeneous fluid in a planar geometry. The hard wall is described by an external potential

$$V_{\text{ext}}(x) = \begin{cases} \infty & x < R \\ 0 & x \geqslant R \end{cases} \tag{12}$$

where x measures the distance from the wall. Since the density profile and therefore the weighted densities only vary in the x-direction we obtain the following expressions using equation (5):

$$n_2(x) = 2\int_{-R}^{R} \mathrm{d}x'\, \rho(x - x')\sqrt{R^2 - x'^2} \tag{13}$$

$$n_1(x) = 2R\int_{-R}^{R} \mathrm{d}x'\, \rho(x - x')\frac{1}{\sqrt{R^2 - x'^2}} \tag{14}$$

$$n_0(x) = \frac{n_1(x)}{2\pi R} + 2R\int \mathrm{d}x'\, \rho'(x - x')\frac{x'}{\sqrt{R^2 - x'^2}}. \tag{15}$$

The density profile can now be solved for, using equations (8), (9), and the results for several bulk densities are shown in figure 1. These profiles are, as expected, very similar to the results obtained in [18] where density profiles were calculated in a circular cavity using the same functional. Furthermore, the contact density $\rho_{\text{w}} = \rho(x = R_+)$ must obey the sum rule $\rho_{\text{w}}\sigma^2 = \beta P$, where P is the bulk pressure of the liquid at density $\rho_0\sigma^2$ [31]. In figure 2, results for ρ_{w} are compared with the bulk pressure obtained from the scaled particle theory equation of state and simulations [32], with excellent agreement.

3.2. The 0D limit

The failure of the original Rosenfeld functional to predict freezing in 3D has been attributed to the divergences that appear in the functional when the 3D density distribution becomes highly peaked [16, 24–26]. As the density distribution approaches a sum of δ-functions, each lattice site can be viewed as a cavity that can hold only one or zero particles. In order for the functional

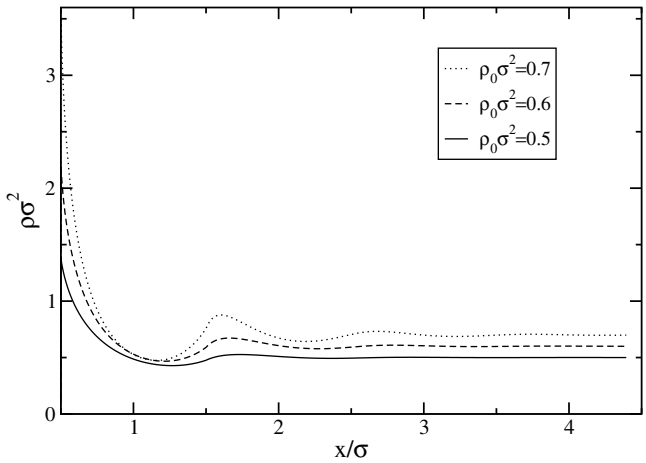

Figure 1. The density profile for hard discs near a hard wall ($\rho_0\sigma^2 = 0.5, 0.6, 0.7$).

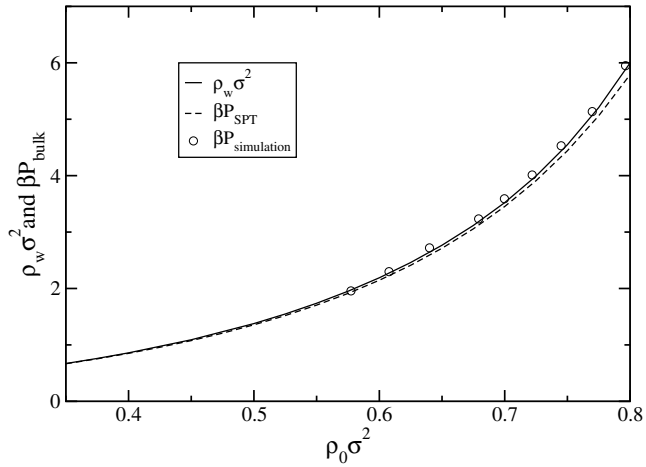

Figure 2. The contact density ρ_w of the 2D liquid compared to the bulk pressure calculated from the SPT equation of state $\beta P_{\text{bulk}} = \rho_0\sigma^2(1 - \rho_0\sigma^2\pi/4)^{-2}$. Results from simulations [32] are shown as circles.

to correctly describe the solid, it must be able to reproduce this 0D limit correctly. Using this idea, several successful improvements have been made to the original Rosenfeld functional that correct the divergent behaviour and yield better dimensional crossover properties, while at the same time preserving the original idea behind the functional [26, 27].

There is no particular reason to expect the 2D functional to exhibit the same divergent behaviour, since the term in $\Phi^{(3D)}$ that gives rise to the divergences is not present in the 2D functional. However, we proceed to test the 2D functional against the exact result for 0D. It can be shown that in 0D the exact excess free energy as a function of the average occupation number in a cavity is [25]

$$f^{(0D)} = N_0 + (1 - N_0)\ln(1 - N_0). \tag{16}$$

As the average occupation number is just the packing fraction, we can calculate the 0D limit of the 2D functional by using a density distribution consisting of a single Gaussian

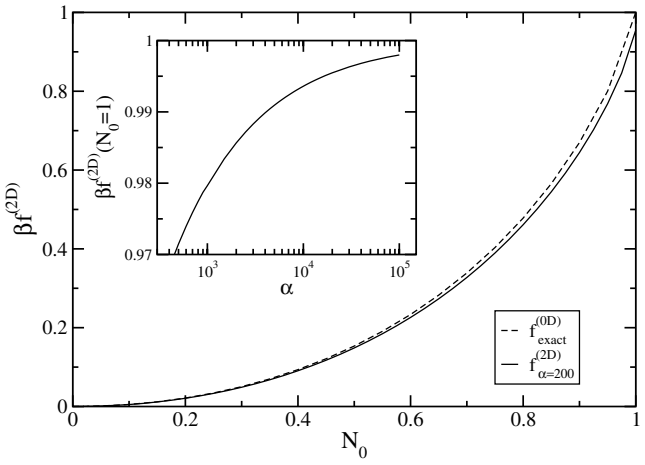

Figure 3. The 0D limit of the 2D functional calculated at $\alpha = 200$ compared to the exact 0D result. The inset shows how the 2D functional at the end-point $N_0 = 1$ approaches 1 as $\alpha \to \infty$.

multiplied by N_0 in the limit $\alpha \to \infty$:

$$\rho(\boldsymbol{r}) = N_0 \frac{\alpha}{\pi} \exp(-\alpha \boldsymbol{r}^2). \tag{17}$$

In figure 3 the results from equations (16) and (17) are compared. The discrepancy may be attributed to an inability of the 2D functional to exhibit perfect dimensional crossover, although the significance of the Gaussian approximation is not yet fully understood. The inset in figure 3 does suggest that as $\alpha \to \infty$ the 0D limit is recovered, but the values of α needed to reproduce the 0D limit are much higher than those observed for the corrected 3D functional [25].

3.3. Phase transitions in a 1D external potential

The general procedure for mapping out the phase behaviour is to solve for the density distribution that minimizes the free energy in each phase and compare the corresponding free energies. For the liquid state, this means using equations (8) and (3)–(5). The solid density distribution is instead given by equation (10) and α is used as variational parameter.

When a periodic external potential is applied to the liquid below the freezing transition, one would expect the liquid to exhibit a symmetry similar to that of the external potential. In the limit of $\beta V_0 \to 0$ the liquid density should approach a cosine form: we find that the amplitude of the perturbed liquid density profile is equal to the result predicted by linear response theory, $\Delta\rho = \beta\rho_0 V_0 S(k)$, where $S(k)$ is the static structure factor and $k = 2\pi/L$ is the wavevector of the external potential. For larger amplitudes of the external potential this is no longer the case, as it would eventually imply regions of negative density. However, when V_0 does become sufficiently large, regions with density approaching zero appear as the liquid density becomes more and more peaked in the troughs of the potential.

As can be seen from figure 4, there is a free energy cost associated with perturbing the liquid for small amplitudes, which negates the drop in free energy obtained from the interaction with the external potential. As V_0 increases and the liquid density becomes sufficiently peaked, $\frac{\delta\beta F_{\text{liquid}}}{\delta V_0}$ approaches -1.

In order to calculate the weighted densities for the solid, we note that both the density and the weight functions in equation (5) are radially symmetric distributions. We cannot, however,

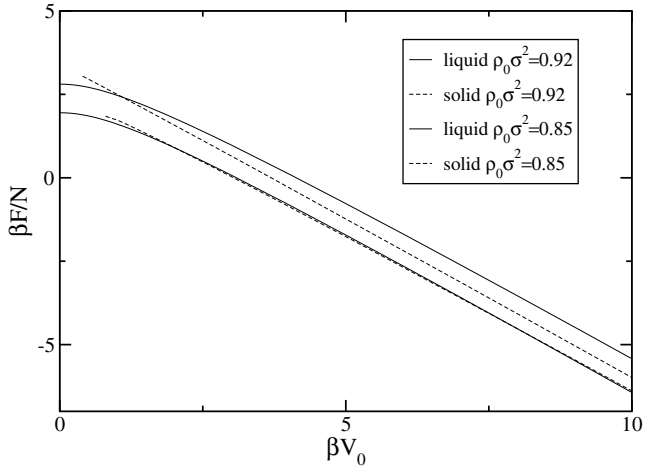

Figure 4. Free energy for the liquid (full curves) and solid (dashed curves) states as a function of βV_0. The re-entrant liquid phase can be seen from the curves for $\rho_0\sigma^2 = 0.85$ as the liquid curve recrosses the solid curve. The solid curves end where the solid state is no longer metastable.

reduce these convolution integrals to radial integrals using the same approach as in 3D [25]. Instead we calculate the weighted densities as Fourier transforms of two radially symmetric functions:

$$n_\gamma(r) = 2\pi \int \mathrm{d}k\, k J_0(kr)\rho(k)w_\gamma(k) \tag{18}$$

using equation (7).

Having the weighted densities for the solid, the free energy per particle can now be calculated. In figure 4 the free energy per particle for the liquid and the solid are plotted against V_0 at two densities. At $\rho_0\sigma^2 = 0.92$ the liquid is stable until $\beta V_0 \simeq 1.0$ where the solid free energy curve crosses the liquid curve. The solid remains the stable phase for higher values of V_0. At $\rho_0\sigma^2 = 0.85$ the solid curve dips below the liquid curve at $\beta V_0 \simeq 2.0$. But at $\beta V_0 \simeq 7.5$ the liquid becomes the stable phase again. The points at which the solid and liquid curves cross are shown in the phase diagram in figure 5. The freezing transition moves to lower densities until $\rho\sigma^2 \simeq 0.837$ where the liquid again becomes more stable than the solid phase. To determine the freezing and melting densities (ρ_f and ρ_m) for a given value of V_0, a double-tangent construction is used. These densities are also shown in figure 5. For $\beta V_0 \to 0$ the solid and liquid curves approach closest packing, signifying no stable solid on a triangular lattice without the influence of an external potential. A metastable solid state is observed for $\rho_0\sigma^2 > 0.95$.

The phase diagram bears a close resemblance to the experimental observations in [5] and supports the notion that the re-entrant liquid phase is only seen for densities just above the minimum in the coexistence curve ($\rho \simeq 0.837$–0.86). It is interesting to note that the liquid density profile corresponding to the bottom of the coexistence curve has regions of nearly zero density with a width of $\sim 2R$. The highest density for which this is possible is $\rho = \sqrt{3}/2 = 0.866$ where $L = 2R$. That seems to support the suggestion that the re-entrant liquid phase is observed when the external potential becomes large enough to quench the correlations between rows of particles and effectively creates 1D stripes of liquid.

However, in contrast to the experimental study our work does not find that the freezing density increases for $\beta V_0 \geqslant 4$. If the number of particles is kept constant and the density is

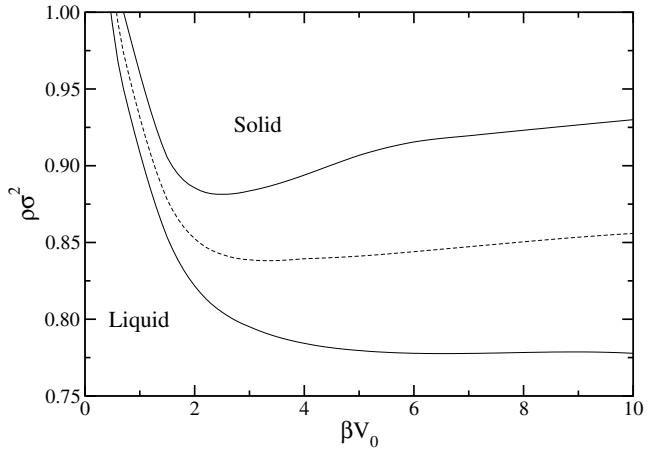

Figure 5. The phase diagram of the hard-disc system in a 1D periodic potential of amplitude V_0. The full curves are the freezing and melting densities. The dashed curve represents the points where the free energy of the solid and liquid states are equal.

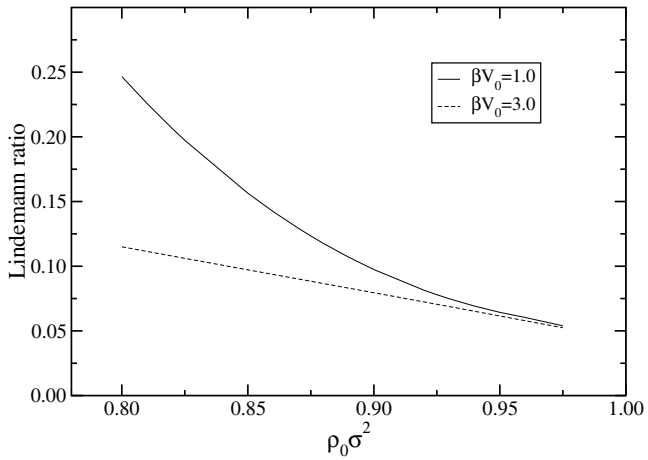

Figure 6. The Lindemann ratio for $\beta V_0 = 1.0$ and 3.0.

fixed between the melting and freezing density, one would expect the system to phase separate, which in an experimental situation would imply that the observed liquid and solid states would overlap in the phase diagram.

We see no evidence for the existence of a critical point in the phase diagram as has been proposed by both theoretical and simulation studies [7, 10]. The transitions between homogeneous liquid, solid and perturbed liquid are first order with non-zero density jumps throughout the phase diagram.

The α-parameter corresponding to the minimum of the solid free energy is used to calculate the Lindemann ratio $(1/\alpha a^2)^{1/2}$ which is shown in figure 6 for different values of the external potential.

4. Discussion

We have applied the KR version of the Rosenfeld functional to a hard-disc fluid in several inhomogeneous situations. The results for adsorption at a hard wall show excellent agreement for the contact densities, and the density profiles closely resemble those obtained from a hard-disc fluid in a spherical cavity [18] using the original Rosenfeld functional and simulations.

The functional also reproduces the 0D limit very well, which indicates good dimensional crossover properties. Any discrepancy that one might infer from the exact 0D result could be a result of the Gaussian density distribution and not due to the functional itself. It would be interesting to repeat this calculation using the newest version of the functional [26, 27], which was derived with this 0D limit in mind.

The phase behaviour of the hard-disc fluid in an external potential showed a remarkable resemblance to recent experimental observations. The phase diagram shows good qualitative agreement and the scale of the external potential matches almost exactly the experimental phase diagram, despite the softer interactions between the particles in experiments. This suggests that not only is the hard-disc fluid an excellent model system for colloidal particles, but the induced phase transitions are governed by entropic rather than energetic effects. Further studies on the temperature dependence of the transitions may shed further light on this.

The proposed microscopic explanation for the induced freezing and melting phenomena involving particles fluctuations is consistent with the density profiles of the perturbed liquid phase that we calculated. In the region of the phase diagram where re-entrant melting is observed, we find that the density profile of the perturbed liquid resembles stripes of liquid separated by stripes with nearly zero density of width $\sim 2R$. By using different symmetries and wavelengths of the external potential, this issue could be further investigated.

Acknowledgments

The authors are grateful to Matthias Schmidt and Joseph M Brader for valuable suggestions and interesting discussions. This work was supported by the National Science Foundation through grant CHE-9800074, and through the Materials Research Science and Engineering Center at the University of Chicago.

References

[1] Chowdhury A, Ackerson B J and Clark N A 1985 *Phys. Rev. Lett.* **55** 833
[2] Loudiyi K and Ackerson B J 1992 *Physica* A **182** 1
[3] Wei Q-H, Bechinger C, Rudhardt D and Leiderer P 1998 *Phys. Rev. Lett.* **81** 2606
[4] Bechinger C, Wei Q H and Leiderer P 2000 *J. Phys.: Condens. Matter* **12** A425
[5] Bechinger C, Brunner M and Leiderer P 2001 *Phys. Rev. Lett.* **86** 930
[6] Loudiyi K and Ackerson B J 1992 *Physica* A **182** 26
[7] Chakrabarti J, Krishnamurthy H R, Sood A K and Sengupta S 1995 *Phys. Rev. Lett.* **75** 2232
[8] Das C, Sood A K and Krishnamurthy H R 1999 *Physica* A **270** 237
[9] Strepp W, Sengupta S and Nielaba P 2001 *Phys. Rev.* E **63** 046106
[10] Chakrabarti J, Krishnamurthy H R and Sood A K 1994 *Phys. Rev. Lett.* **73** 2923
[11] Das C, Krishnamurthy H R and Sood A K 1998 *Phys. Rev.* B **58** 1998
[12] Frey E, Nelson D R and Radzihovsky L 1999 *Phys. Rev. Lett.* **83** 2977
[13] Rosenfeld Y 1989 *Phys. Rev. Lett.* **63** 980
[14] Rosenfeld Y, Levesque D and Weis J-J 1990 *J. Chem. Phys.* **92** 6818
[15] Rosenfeld Y 1990 *Phys. Rev.* A **42** 5978
[16] Kierlik E and Rosinberg M L 1990 *Phys. Rev.* A **42** 3382
[17] Kierlik E and Rosinberg M L 1991 *Phys. Rev.* A **44** 5025
[18] Kim S-C, Nemeth Z T, Heni M and Löwen H 2001 *Mol. Phys.* **99** 1875

[19] Rosenfeld Y 1994 *Phys. Rev.* E **50** R3318
[20] Schmidt M, Löwen H, Brader J M and Evans R 2000 *Phys. Rev. Lett.* **85** 1934
[21] Brader J M, Evans R, Schmidt M and Löwen H 2002 *J. Phys.: Condens. Matter* **14** L1
[22] Schmidt M 2001 *Phys. Rev.* E **63** 050201(R)
[23] Schmidt M and von Ferber C 2001 *Phys. Rev.* E **64** 051115
[24] Rosenfeld Y, Schmidt M, Löwen H and Tarazona P 1996 *J. Phys.: Condens. Matter* **8** L557
[25] Rosenfeld Y, Schmidt M, Löwen H and Tarazona P 1997 *Phys. Rev.* E **55** 4245
[26] Tarazona P 2000 *Phys. Rev. Lett.* **84** 694
[27] Schmidt M 2001 *Phys. Rev.* E **84** 694
[28] Jaster A 1999 *Phys. Rev.* E **59** 2594
[29] Phan S, Kierlik E, Rosinberg M L, Bildstein B and Kahl G *Phys. Rev.* E **48** 618
[30] Gonzalez A, White J A and Evans R 1997 *J. Phys.: Condens. Matter* **9** 2375
[31] Henderson J R 1992 *Fundamentals of Inhomogeneous Fluids* (New York: Dekker) p 23
[32] Hoover W G and Alder B J 1968 *J. Chem. Phys.* **46** 686